Supporting Information

Air-sea interactions on Titan: effect of radiative transfer on the lake evaporation and atmospheric circulation

Audrey Chatain[1,2], Scot C.R. Rafkin[1], Alejandro Soto[1], Ricardo Hueso[2] and Aymeric Spiga[3]

[1] Department of Space Studies, Southwest Research Institute (SwRI), 1050 Walnut Street, Suite 300, Boulder, CO 80302, USA

[2] Departamento de Física Aplicada, Escuela de Ingeniería de Bilbao, Universidad del País Vasco/Euskal Herriko Unibertsitatea (UPV/EHU), Plaza Ingeniero Torres Quevedo 1, 48013 Bilbao, Spain

[3] Laboratoire de Météorologie Dynamique/Institut Pierre-Simon Laplace (LMD/IPSL), Centre National de la Recherche Scientifique (CNRS), Sorbonne Université, 4 place Jussieu, Tour 45-55 3e étage, 75252 Paris, France

This document details additional results of the improved mtWRF model discussed in the paper "*Air-sea interactions on Titan: effect of radiative transfer on the lake evaporation and atmospheric circulation*" published in The Planetary Science Journal in 2022 by the above mentioned authors. The paper focuses on the main effects of radiations on the resulting solution, which are of main interest for the general reader. However, for readers in search of more quantitative results, we added detailed information here on the effects of the initial lake temperature (S1), the depth of the lake mixed layer (S2) and the background wind (S3).

S1- Initial lake temperature: control of an initial methane plume

The lakes temperature on Titan is not known. However, Rafkin and Soto (2020) showed that lakes are likely to be much colder than the land due to long-term evaporative cooling. We tested different values for the initial lake temperature (93.47 K, 90.5 K and 88 K) and we found that the stabilized regime after 2-3 days is identical in all cases. Only the initialization phases are different.

Figure S1.1 shows the initialization phase for the three different simulations: one starting with a lake at 93.47 K (S-G), one at 90.5 K (S-A) and one at 88 K (S-I). A significant methane plume is formed in the warmer lake case. This is due to a high latent heat flux (see Figure S1.2) that leads to intense evaporation of methane from the lake. Methane being lighter than di-nitrogen (the main compound of the atmosphere), it moves up and forms the vertically extended plume creating a circulation with winds from the land to the lake at the surface, and the reverse at the top of the plume. As time passes, the air above the lake becomes colder and more stable due to the strong evaporation of methane, and the central plume weakens. After a few hours, the circulation starts to reverse at the surface, going from the cold dense air over the lake to the warmer air above the land creating a sea breeze. Soon, the sea breeze dominates the initial plume circulation and extends over land. This formation of plumes from a 'warm' lake has been previously observed in Rafkin and Soto (2020).

In the case of a lake with initial temperature equal or inferior to the equilibrium temperature there is no such a plume. On the opposite, the colder the lake, the less methane vaporizes in the initial phase due to a smaller latent heat flux. In the 88 K lake case, the very low initial latent heat flux cannot compensate the sensible heat flux and the radiative fluxes, which lead to a warming of the lake, up to the equilibrium temperature, when the latent heat flux compensates in average the heating fluxes. At the beginning of S-I, the temperature difference between the cold lake and the land being larger than in S-A, the formed sea breeze is stronger.

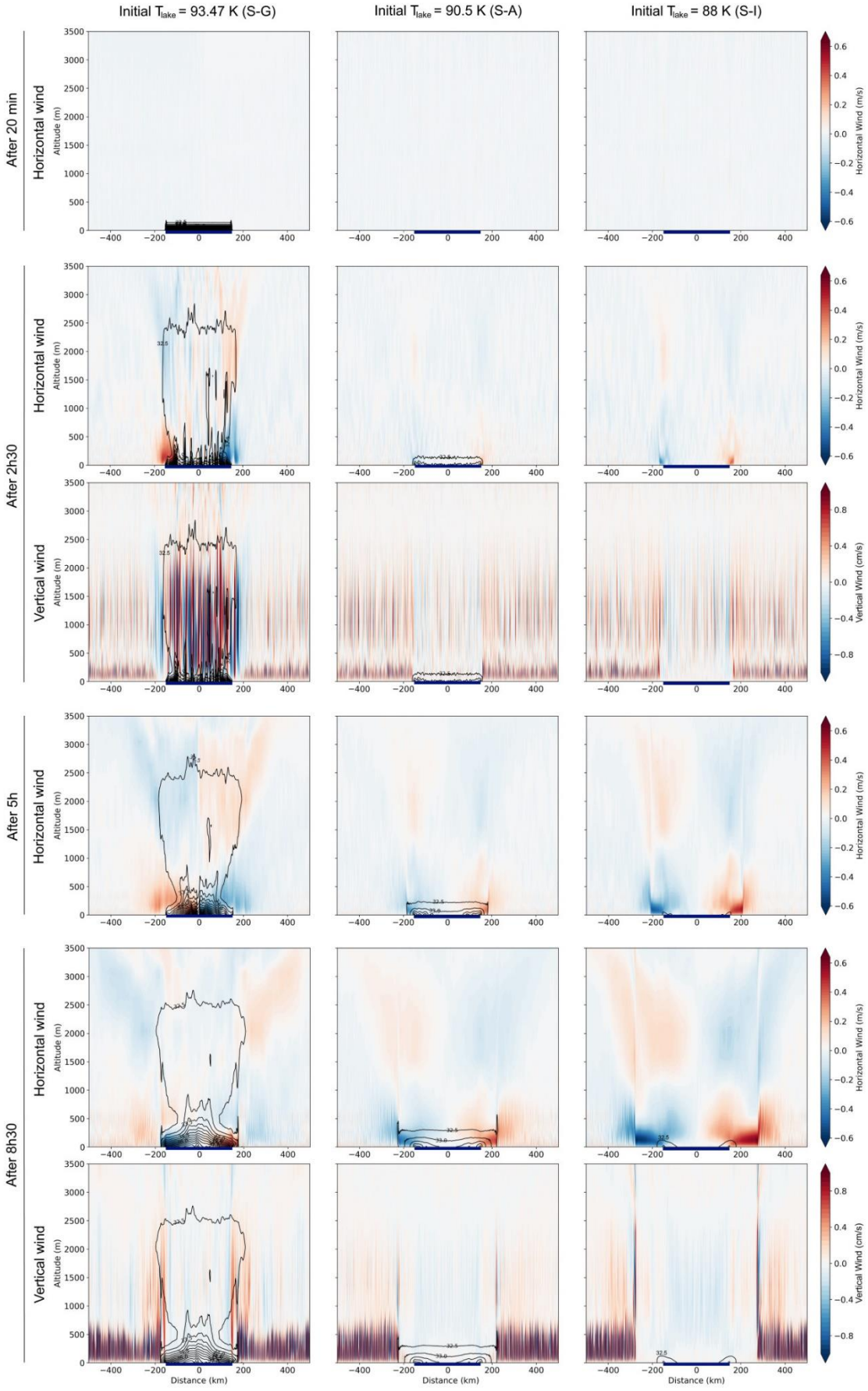

Figure S1.1: Horizontal (and vertical) wind along the 2D simulation at different simulation times: after 20 min, 2h30, 5h and 8h30. Contours give the methane mixing ratio every 0.5 g.kg^{-1}. Plots are obtained with simulations S-G ($T_{lake,ini}$ = 93.47 K), S-A (90.5 K) and S-I (88 K) starting at 00h. The dark blue line indicates the lake position.

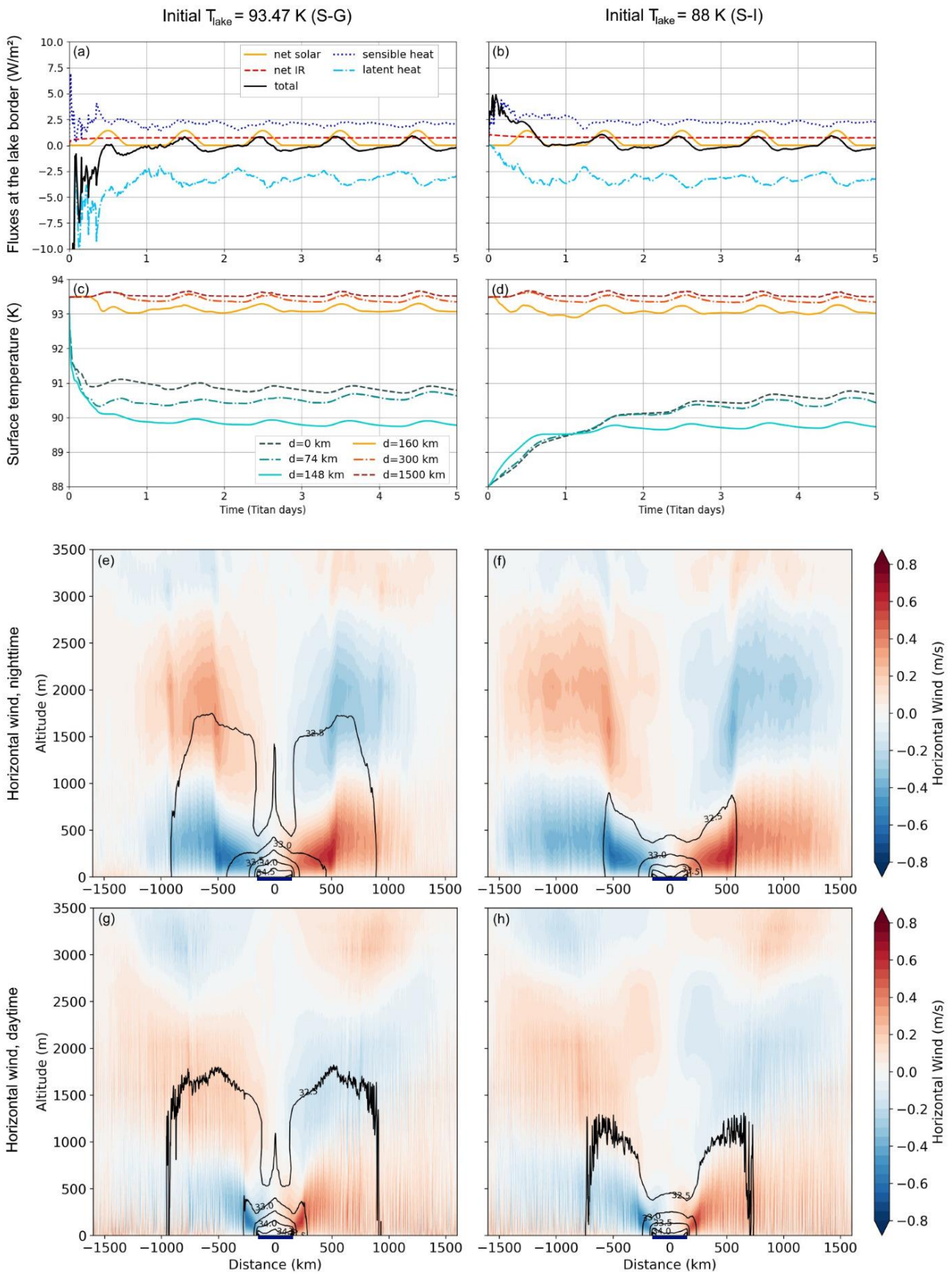

Figure S1.2: Output results from S-G ($T_{lake,ini}$ = 93.47 K) and S-I (88 K). (a,b) Time evolution of energy fluxes at the shore (to compare to Figure 4e). (c,d) Time evolution of surface temperature (to compare to Figure 3e). (e,f,g,h) Horizontal wind along the 2D simulation. Contours give the methane mixing ratio every 0.5 g.kg^{-1}. Average over 1-3 am and 1-3 pm on the 4th day (to compare to Figure 5).

Finally, we conclude that the stabilized regime for all of the three cases is nearly exactly the same (see Figure S1.2). The only small differences are due to remnants of the different initial phases. In particular, remnants of the methane plume are observed in the methane mixing ratio distribution in the stabilized phase of S-G. Also, more methane is found in the atmosphere of S-G in the stabilized regime, and less in the case of S-I, because of the different production rates of methane vapor in the initial phase. Methane vapor is accumulated over the course of the simulation, but in the stabilization phase, all simulations have an identical production rate of methane at the surface of the lake. Finally, the maximal extension of the sea breeze (not the position of the front) is bigger for S-I because the initial stronger sea breeze.

In conclusion, the lake temperature is totally determined by the system and is therefore not a free parameter. If a seasonal or geologic phenomenon changes the lake temperature from its equilibrium value on Titan, it would tend to go back to it by adapting the methane evaporation rate.

S2- Depth of the lake mixed layer: control of the inertia to (diurnal and seasonal) variations

This section investigates the effect of the depth of the lake mixed layer. Previous sections have focused on a shallow mixed layer of 1 m. However, lakes on Titan can have a larger depth, possibly over 100 m (Mastrogiuseppe et al., 2019), and therefore the upper mixed layer could possibly be much bigger than 1 m. In particular, pure methane lakes have an equilibrium phase very stratified, with colder layers at the bottom (Tokano, 2005). Consequently, the nighttime and winter time cooling of the top of the lake leads to an overturn in the lake stratification, and so to a deeper mixed layer. On the opposite, the lake stratigraphy is likely to be more stable (i.e. with a shallow mixed layer) during the day and the summer, when the top of the lake is heated by the sun. However, this is not totally straightforward as a higher insolation also triggers a stronger cooling by evaporation. Besides, non-pure methane lakes (potentially mixed with ethane and/or nitrogen) and lakes with a composition varying with depth (Steckloff et al., 2020) could have a different equilibrium stratigraphy to cold at the bottom and warm at the top triggering different values for the mixed layer depth (Tan et al., 2015).

Simulations S-J (10 m) and S-K (100 m) tackle the influence of mixed layer depth in comparison to the reference case S-A (1 m). The resulting outputs of the three simulations are mostly identical. The wind circulation (sea breeze) is exactly the same, with the same spatial extent, the same intensity and the same diurnal evolution. The only difference is situated at the shores. Indeed, the chosen initial lake temperature is the stabilized temperature in the central part of the lake. However, the lake shores are always colder, and in all previously studied cases, the lake temperature at the shores decreased during 1 to 2 days to reach a colder stabilized temperature. However here, deeper mixed layer cases induce a larger inertia and a longer time to reach the stabilized lower temperature. As a consequence, S-J and S-K did not reach the stabilized phase after 5 simulations days (see Figure S2 a-b to compare to Figure 3e in the paper). Lakes with deeper mixed layers take longer times to accommodate to external heating/cooling variations. In particular, no diurnal variation on the lake temperature is observed in the 100 m case (S-J), while a very slight diurnal variation is observed in the 10 m case (S-K). However, notable variations happen in the 1 m case (S-A), in particular representative of shallow and possibly transient lakes (MacKenzie et al., 2019).

The fact that the S-J and S-K cases did not reach a stabilized phase after 5 days is also observed on the energy fluxes at the shore (see Figure S2 c-d, to compare to Figure 4e). In these two cases, the total flux is not zero, and is negative, explaining why lakes are still cooling down after 5 days. The 10 m case (S-J) is likely to reach the stabilized phase in a few more days, but the 100 m case (S-K) does not show any attenuation of the cooling process after 5 days. All other things being equal, a rough estimate is that the 10 m case would take 10 times longer to stabilize than the 1 m case (so ~10 Titan days), and the 100 m case would take 100 times longer than the 1 m case (~100 days). The negative total flux at the shores is due to a higher latent heat flux in absolute value when the mixed layer depth increases from 1 to 10 to 100 m. All other fluxes stay the same, with just a slight decrease of the sensible heat and the IR flux due to the higher temperature of the lake.

The consequence of a longer time to reach equilibrium is then a higher latent heat flux during longer periods of time, and therefore more evaporation of methane. In these simulations, the initial temperature of the

central part of the lake is very close to its equilibrium temperature, but this is less the case on the shores. This is in particular why higher quantities of methane vapor are observed at the lake shores and spread in the atmosphere (see Figure S2 e-f to compare to Figure 3i).

The main conclusion here is that a deeper mixed layer acts as a higher inertia to changes in the lake, while shallower mixed layers and shallow lakes react more strongly to the effects of the daily cycle. This impacts mostly the lake temperature variations. Another consequence is the higher capacity of the lake to inject methane in the atmosphere for a given environmental change (eg. seasons). On the other hand, the sea breeze structure stays exactly the same independently on the depth of the lake mixed layer.

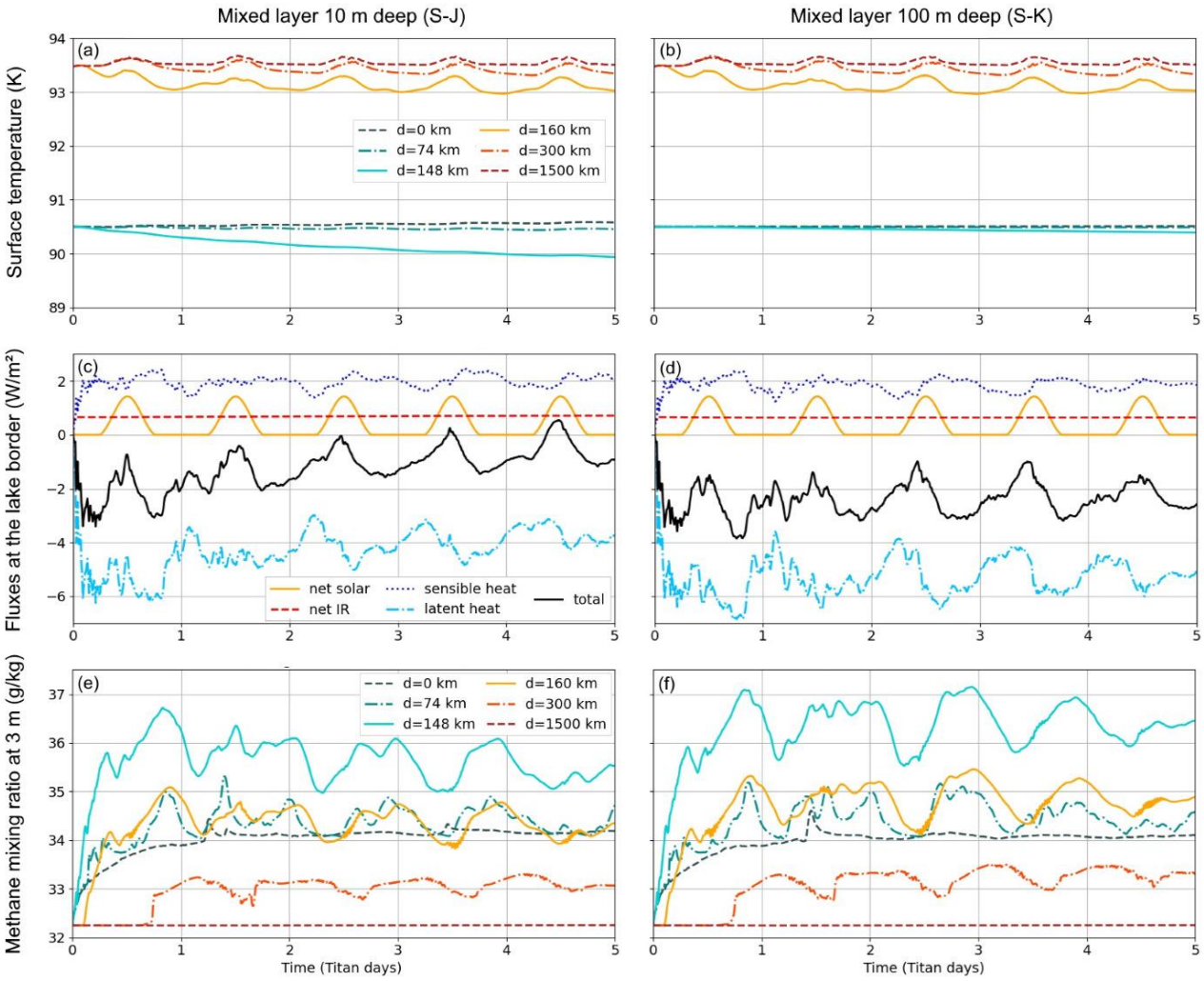

Figure S2: (a-b) Evolution of the surface temperature at different locations, to compare to Figure 3e in the paper. (c-d) Evolution of the energy fluxes on the shore, to compare to Figure 4e. (e-f) Evolution of the methane mixing ratio at different locations, to compare to Figure 3i. Results obtained with lakes of different depths: 10 m (S-J) and 100 m (S-K).

S3- Background winds: asymmetry of the sea breeze

The addition of a background wind is investigated in this section. We ran two simulations, with background winds of 1 $m.s^{-1}$ (S-L) and 3 $m.s^{-1}$ (S-M). These two cases have been previously studied in Rafkin and Soto (2020) with the previous version of the model, without radiation. We update those numerical experiments here. Although wind values of 1 and 3 $m.s^{-1}$ are high for the sluggish atmosphere of Titan these are the initial background winds at all altitudes in the model domain and the surface friction quickly reduces the winds near the surface. The use of background winds quickly moves lake-induced wind structures and methane vapor towards one border of the simulation box. For this reason, we increased the simulation box to 6400 km (with the 300 km lake at the center), and reduced the simulation time to 4 Titan days. We kept periodic boundary conditions and did not observed any cyclic contamination in this configuration.

The nighttime and daytime wind circulations on the 4^{th} day of simulation in the 1 $m.s^{-1}$ and 3 $m.s^{-1}$ background wind cases are presented in Figure S3.1, to compare to the case without background wind in Figure 5 in the paper. With background winds, the sea breeze still forms, but with a strongly asymmetric shape. Its vertical and horizontal extends are limited by the background wind. For a background wind coming from the left, the sea breeze merges with the background wind on the right side, while its extension on the left side is limited by a net collision with the background wind, at -500 km from the lake center in the 1 $m.s^{-1}$ case, and at -200 km in the 3 $m.s^{-1}$ case. This frontier is coincident with a strong vertical wind, which is very localized at night, and horizontally extended over up to 200 km during the day in S-L (1 $m.s^{-1}$). As a direct consequence of the asymmetric wind circulation, the methane vapor is spread far inland in the direction of the background wind, while it is accumulated and elevated at the collision line on the left. The vertical extent of the sea breeze is much more limited in the 3 $m.s^{-1}$ background wind case.

To get more insights on the processes created by the interaction with the environment winds, Figure S3.2 compares the evolution with time of winds, fluxes, methane mixing ratio and temperatures for S-A (0 $m.s^{-1}$), S-L (1 $m.s^{-1}$) and S-M (3 $m.s^{-1}$). The same conclusions as for Figure S3.1 can be drawn for the wind: the sea breeze is deformed by the background wind. It is more restricted to the shore on the left side (over only 10s of kilometers for S-M). Stronger winds are observed at the surface, especially above the lake, and even in the direction opposite to the background wind. These are explained by a higher land-lake temperature difference. At 230 m, the sea breeze is strongly weakened in the 3 $m.s^{-1}$ case. It cannot hold winds reversed to the background wind, but it slows them down. The sensible and latent heat fluxes exactly follow the surface wind pattern (in absolute value) above the lake. They still have a diurnally varying trend in S-L, but they are mostly driven by random wind gusts in S-M. The fluxes are globally slightly higher in cases with background winds, especially on the left shore. As a consequence, more methane vapor is produced, mainly over the left shore. The newly formed cold moist air is then spread over land following the winds. Another consequence of the higher latent heat flux is an enhanced cooling of the lake of ~0.5 K.

In conclusion, a background wind deforms the sea breeze structure, quickly diffuses cold air over land in the background wind direction and creates an updraft front on the other side. Surface winds are also increased, leading to more methane evaporation and an accentuated cooling of the lake.

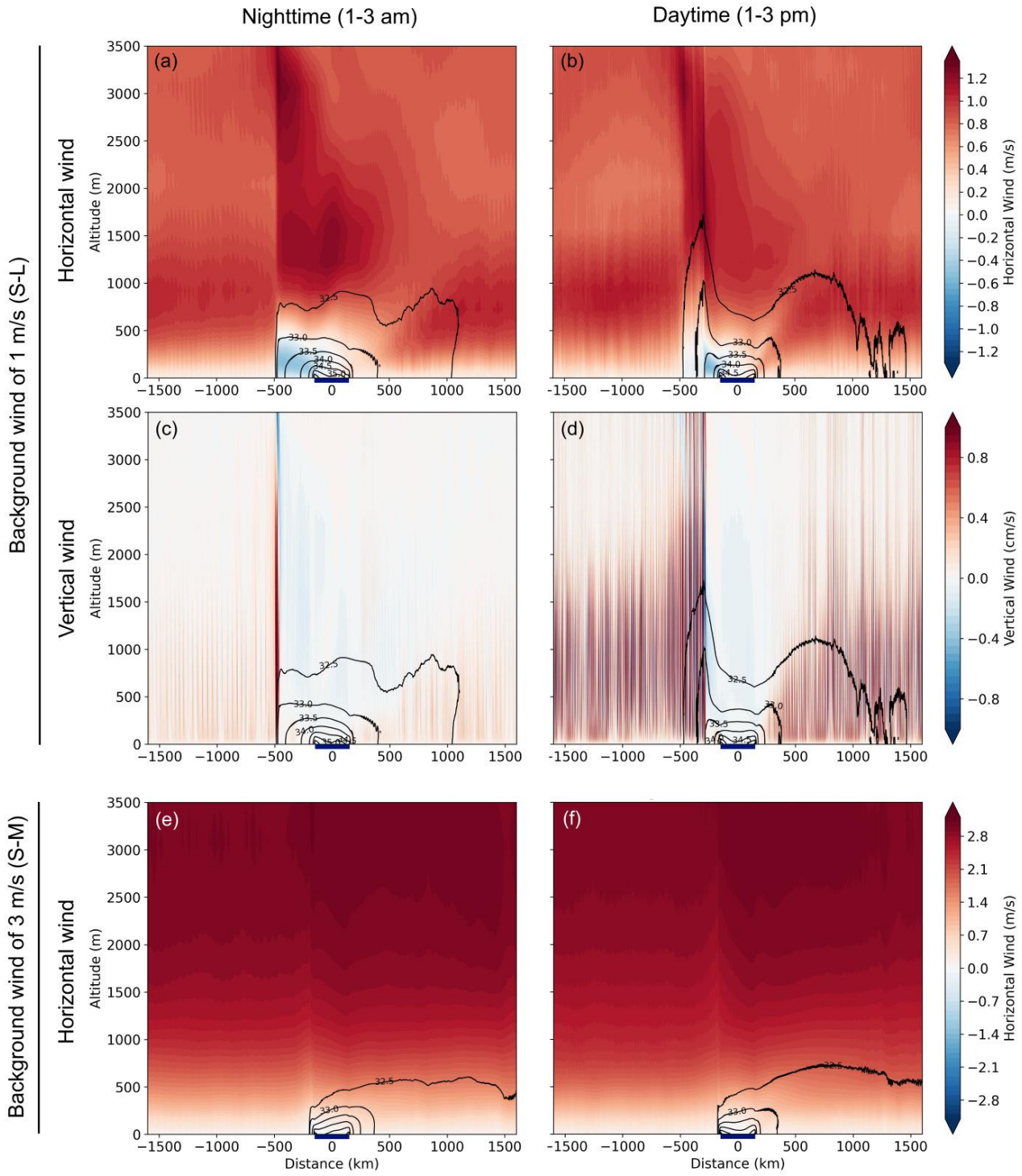

Figure S3.1: Horizontal and vertical wind along the 2D simulation. Contours give the methane mixing ratio every 0.5 g.kg^{-1}. Average over 1-3 am and 1-3 pm on the 4th day for simulations S-L (background wind of 1 m.s^{-1}) and S-M (3 m.s^{-1}). To compare to Figure 5 in the paper. The dark blue line indicates the lake position.

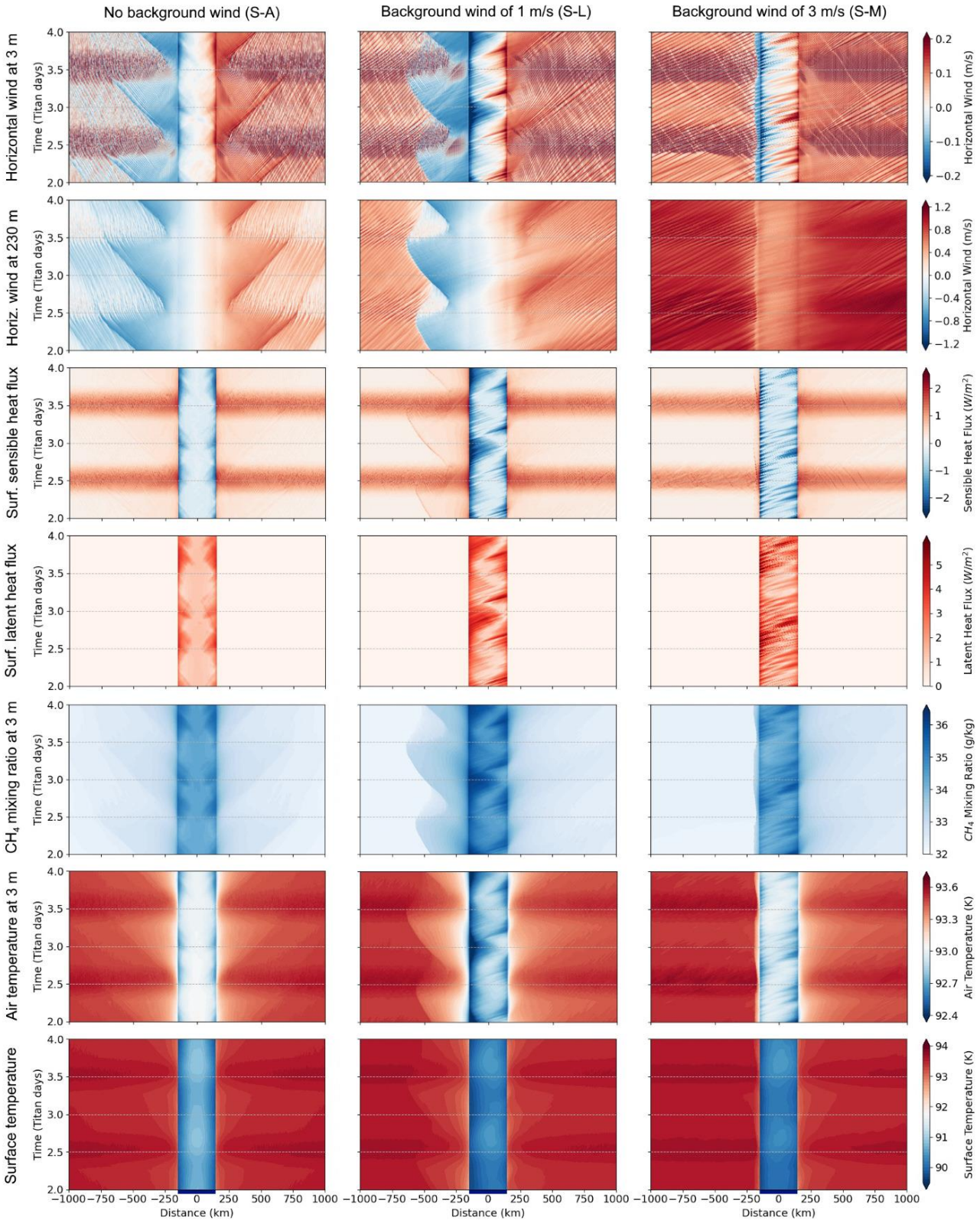

Figure S3.2: Evolution with time of the horizontal wind at 3 m and 230 m, the surface sensible and latent heat fluxes, the methane mixing ratio at 3 m, and the temperature at 3 m and at the surface, for simulations S-A (no background wind), S-L (background wind of 1 m.s^{-1}) and S-M (3 m.s^{-1}). The dark blue line indicates the lake position.

References

MacKenzie, S.M., Barnes, J.W., Hofgartner, J.D., Birch, S.P.D., Hedman, M.M., Lucas, A., Rodriguez, S., Turtle, E.P., Sotin, C., 2019. The case for seasonal surface changes at Titan's lake district. Nat. Astron. 3, 506–510. https://doi.org/10.1038/s41550-018-0687-6

Mastrogiuseppe, M., Poggiali, V., Hayes, A.G., Lunine, J.I., Seu, R., Mitri, G., Lorenz, R.D., 2019. Deep and methane-rich lakes on Titan. Nat. Astron. 3, 535–542. https://doi.org/10.1038/s41550-019-0714-2

Rafkin, S.C.R., Soto, A., 2020. Air-sea interactions on Titan: Lake evaporation, atmospheric circulation, and cloud formation. Icarus 351, 113903. https://doi.org/10.1016/j.icarus.2020.113903

Steckloff, J.K., Soderblom, J.M., Farnsworth, K.K., Chevrier, V.F., Hanley, J., Soto, A., Groven, J.J., Grundy, W.M., Pearce, L.A., Tegler, S.C., Engle, A., 2020. Stratification Dynamics of Titan's Lakes via Methane Evaporation. Planet. Sci. J. 1, 26. https://doi.org/10.3847/PSJ/ab974e

Tan, S.P., Kargel, J.S., Jennings, D.E., Mastrogiuseppe, M., Adidharma, H., Marion, G.M., 2015. Titan's liquids: Exotic behavior and its implications on global fluid circulation. Icarus 250, 64–75. https://doi.org/10.1016/J.ICARUS.2014.11.029

Tokano, T., 2005. Thermal structure of putative hydrocarbon lakes on Titan. Adv. Sp. Res. 36, 286–294. https://doi.org/10.1016/j.asr.2005.03.051